SONOELASTIC DETERMINATION OF THE KNEE CARTILAGE ELASTICITY

LIGIA MUNTEANU[1], LUCIANA MAJERCSIK[2], VALERICA MOSNEGUTU[1]

Abstract. Sonoelasticity and Doppler imaging are applied in this paper to detect the damage process of the knee cartilage. The cartilage is a firm, thick, slippery tissue that acts as a protective cushion between bones. It is present on the ends of the bones and at the back of the patella and provides low friction in distributing of loads and maximal consistency between the joint surfaces. Sonoelasticity utilizes an external source to vibrate the knee at low frequency. Vibrations and local motions induced in the cartilage are detected and visualized by Doppler ultrasound by real-time images of normal vibration eigenmodes. The vibration images depend on the vibration frequency, the cartilage structure and elastic properties. Doppler ultrasound detects the vibration amplitudes from the echoes reflected from the cartilage and surrounding tissues. The prediction of small inhomogeneities in the damaged cartilage is compared with theoretical/ experimental data available in literature.

Key words: sonoelasticity, Doppler effect, human knee, cartilage.

1. INTRODUCTION

The key of sonoelasticity is low frequency (about 100 Hz) vibrations for visualizing the human tissues. An external source is used to vibrate the tissue and a Doppler ultrasound detects low-frequency vibrations and motion of the tissue giving real-time vibration images which depend on the tissue structure and their elastic properties. Vibration images of the tissue show all disturbances in the normal vibration eigenmodes generated by damages in the knee structure [1, 2]. In this paper, the human knee elasticity is evaluated from the point of view of the cartilage behavior during the knee flexion and extension. The ability of the sonoelasticity to predict the small inhomogeneities in the tissue through the vibration images, is confirmed both theoretically and experimentally [3–5].

Based on the significant changes in the vibration response of the cartilage for different loadings, the relationship between the loading and the normal modes of vibrations is performed by using an elastic model of the knee [6–9]. This model introduces 12 degrees of freedom described the movement of the patella relative to

[1] Institute of Solid Mechanics of the Romanian Academy, Bucharest
[2] Technical University of Civil Engineering, Bucharest, Romania

Ro. J. Techn. Sci. – Appl. Mechanics, Vol. 62, N° 1, P. 57–67, Bucharest, 2017

the thigh. The cartilage elasticity cannot be described outside the behavior of components of the knee. The knee is a unitary system. This model is ready to evaluate the stiffness of the cartilage by measurements done on the medial and lateral faces of the patella, the medial and lateral faces on the patellar surface of the femur, and the medial and lateral femoral condyles and tibial plateau.

Conventional Doppler analysis cannot be applied when the frequency of motion approaches the Doppler frequency [10]. If an ultrasonic wave is applied to a set of particles which form a tissue, the signal returned by the *k*-th particle has the form

$$s_k = a_k \cos\left(\omega_0 t - 4\pi r_k / \lambda_0\right), \tag{1}$$

where ω_0 is the angular frequency, λ_0 is the wavelength, a_k is the amplitude of the reflected wave and r_k is the distance between the transducer and the tissue's particle.

The Doppler ultrasound determine the vibration amplitude from the signals reflected from the oscillating tissue.

2. ELASTIC MODEL OF THE KNEE

Articular cartilage is a composite material with interesting elastic properties. The tissue contains about 70 to 85% water and in rest, proteoglycans and collagen.

The cartilage is a component in the knee that includes the end of the femur, the top of the tibia, articular cartilage AC, meniscus cartilage, four ligaments, and two tendons: the anterior cruciate ligament ACL, the posterior cruciate ligament PCL, the medial collateral ligament MCL, the lateral collateral ligament LCL, the quadriceps tendon (QT) and the patellar tendon (PTL) – Fig. 1 [6, 7].

The apparent space between the bones is actually occupied by articular cartilage AC. The articular cartilages (AC) act bearing surfaces and the meniscus as mobile bearings. There are large muscles in the front of the thigh (the quadriceps muscles QM) that straighten the knee (extension). The large muscles in the back of the thigh (the hamstrings) bend the knee (flexion). The quadriceps tendon (QT) and the patellar tendon (PTL) surround the patella and helps its mechanical motion and also functions as a cap for the condyles of the femur. Details on the articular cartilage in the normal human knee are found in [11–14].

The integrity of the intact or damaged cartilage is evaluated by measurements of stiffness on the medial and lateral faces of the patella, the medial and lateral faces on the patellar surface of the femur, and the medial and lateral femoral condyles and tibial plateau (Fig. 2). The measurements we use in this article are available in [11].

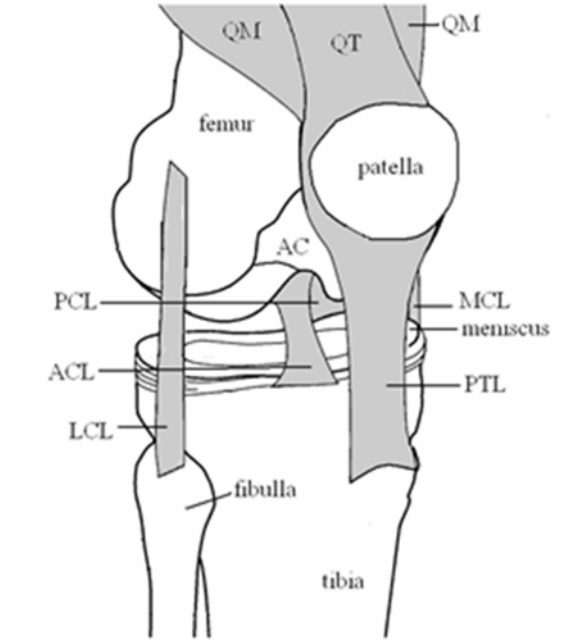

Fig. 1 – Schematic of the knee components [6].

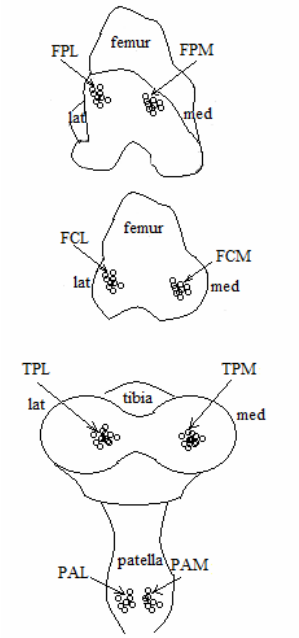

Fig. 2 – Measurements of cartilage stiffness in the knee.

Position of the knee joint is described by local coordinate systems for each bone (Fig. 3). The femoral (x_f, y_f, z_f) and the tibial (x_t, y_t, z_t) coordinate systems have the origin located at the midpoint of the line between the medial and lateral femoral epicondyles and the medial lateral tibial condyles, respectively. The origin of the patellar coordinate system and the patellar (x_p, y_p, z_p) is in the centroid of the patella. The medial x, posterior y, and superior z directions are positive and parallel to (x, y, z). The (x, y) plane is defined as the coronal plane and (y, z) as the sagittal plane. In the global system, a point belonging to knee joint articular surface Γ is denoted by (x, y, z). In the local coordinate systems, a point belonging to Γ is defined by (x'_L, y'_L, z'_L) with L the local system. The transformation from (x'_L, y'_L, z'_L) to (x, y, z) is given by

$$x_i = u_i + R_{ik} x'_{kL}\,, \tag{2}$$

where R_{ik} are the elements of the rotation matrix $\mathbf{R} = \mathbf{R}(z,\varphi)\mathbf{R}(x,\theta)\mathbf{R}(z,\psi)$ with

$$\mathbf{R}(z,\psi) = \begin{bmatrix} \cos\psi & -\sin\psi & 0 \\ \sin\psi & \cos\psi & 0 \\ 0 & 0 & 1 \end{bmatrix}, \quad \mathbf{R}(x,\theta) = \begin{bmatrix} 1 & 0 & 0 \\ 0 & \cos\theta & -\sin\theta \\ 0 & \sin\theta & \cos\theta \end{bmatrix}, \tag{3}$$

$$\mathbf{R}(z,\varphi)=\begin{bmatrix}\cos\varphi & -\sin\varphi & 0\\ \sin\varphi & \cos\varphi & 0\\ 0 & 0 & 1\end{bmatrix},$$

and ***u*** is the translation vector.

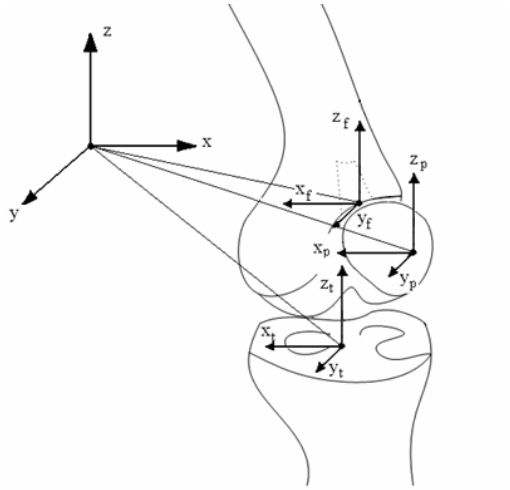

Fig. 3 – The global and local systems of coordinates [6].

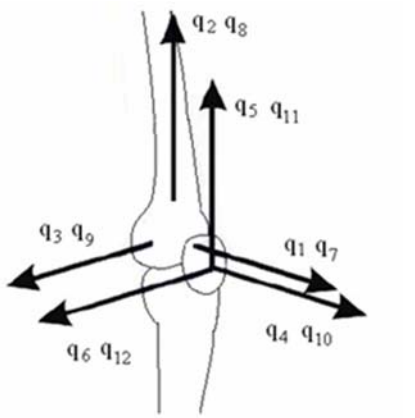

Fig. 4 – Degrees of freedom [6].

We suppose that 12 degrees of freedom $\mathbf{q}=\{q_1,q_2,q_3,...q_{12}\}$ described the movement of the patella relative to the thigh (Fig. 4). These degree of freedom are defined by anterior-posterior translation of the shank relative to the thigh q_1, proximal-distal translation of the shank relative to the thigh q_2, medial-lateral translation of the shank relative to the thigh q_3, anterior-posterior translation of the patella relative to the thigh q_4, proximal - distal translation of the patella relative to the thigh q_5, medial-lateral translation of the patella relative to the thigh q_6, varus-valgus rotation of the knee q_7, internal-external rotation of the knee q_8, flexion-extension of the knee q_9, patellar rotation q_{10}, patellar tilt q_{11}, patellar flexion-extension q_{12}.

The patellar tendon is inextensible and that interpenetration between the boundaries of the patella and the patellar surfaces of the femur can be neglected. These two assumptions define three holonomic constraints for movement of the patella on the femur. These three constraints can be combined with the six force and moment equilibrium equations for the patella to yield a set of six non-linear algebraic equations for patello-femoral mechanics

$$p_i\left(q,F_Q\right)=0,\quad i=1,2,...,6\,, \tag{4}$$

where F_Q is the force magnitude applied by the quadriceps tendon to the patella.

The dynamical equations of the knee motion can be written as

$$\mathbf{A}(\mathbf{q})\ddot{\mathbf{q}} + \mathbf{C}(\mathbf{q},\dot{\mathbf{q}}) + \mathbf{M}_m(\mathbf{q})\mathbf{F}_m + \mathbf{M}_l(\mathbf{q})\mathbf{F}_l + \mathbf{T}(\mathbf{q},\dot{\mathbf{q}}) = 0\,, \tag{5}$$

where $\mathbf{A}(\mathbf{q})$ is the mass matrix, $\mathbf{C}(\mathbf{q},\dot{\mathbf{q}})$ is the vector containing the Coriolis and centrifugal forces and torques arising from the motion of the thigh, $\mathbf{F}_m$ is the vector of forces applied by two muscles (QM, QT), $\mathbf{M}_m(\mathbf{q})$ is the matrix describing the moment arms of applied muscle forces, $\mathbf{F}_l$ is the vector containing the forces applied by four ligaments and two tendons, $\mathbf{M}_l(\mathbf{q})$ is a matrix describing the moment arms of the knee ligament and tendon forces, and $\mathbf{T}(\mathbf{q},\dot{\mathbf{q}})$ is the vector of external torques applied at the joints.

Equations (4) and (5) define a system of 12 nonlinear differential and algebraic equations in 12 unknowns.

We model an inhomogeneity in the cartilage as an elastic inhomogeneity inside a homogeneous elastic medium. The cartilage stiffness is modeled by $\mathbf{A}$, $\mathbf{C}$, $\mathbf{M}_m$, $\mathbf{M}_l$ and $\mathbf{T}$ except with a small area around a point P_0 characterized by $\mathbf{A} + \delta\mathbf{A}$.

The unknowns q_i, $i = 1,2,...,12$, are found by applying the Linear Equivalence Method [15, 16]. This method is used to solve nonlinear differential equations with arbitrary Cauchy data

$$\frac{\mathrm{d}\mathbf{x}}{\mathrm{d}t} = \mathbf{f}(\mathbf{x}), \quad \mathbf{x} = \begin{pmatrix} x_1 \\ x_2 \\ \dots \\ x_n \end{pmatrix}, \quad \mathbf{f}(\mathbf{x}) = \begin{pmatrix} f_1(\mathbf{x}) \\ f_2(\mathbf{x}) \\ \dots \\ f_n(\mathbf{x}) \end{pmatrix}$$

$$\mathbf{x}(t_0) = \mathbf{x}_0, \quad t_0 \in I \subset \mathbb{R},$$

where $f_j(\mathbf{x}) = \sum_{|\nu|\geq 1} f_{j\nu}\,\mathbf{x}^{\boldsymbol{\nu}}$, and $f_{j\nu}$ are defined on a real interval I. $\boldsymbol{\nu} = (\nu_1, \nu_2, \dots \nu_n)$ is a multi-indices vector with n components, and $\mathbf{z}^{\boldsymbol{\nu}} = \prod_{j=1}^{n} z_j^{\nu_j}$.

3. THE CASE OF AN INTACT CARTILAGE

The forces in the cartilage are evaluated from solutions of equations (4) and (5) as

$$F_i = \sum_{k=1,\dots,12} \frac{a_{ki}}{b_{ki}} \sin(b_{ki} + d_{ki}c_{ki})q_k + \dots + \frac{3a_{ki}^3}{16b_{ki}\left(1 + a_{ki}^2\right)}\left[\frac{c_{ki}}{d_{ki} + c_{ki}} \sin(3b_{ki} + c_{ki})q_{ki} \dots\right.$$

$$+\frac{3c_{ki}}{d_{ki}+c_{ki}}\left(\sin(b_{ki}+5c_{ki})S_{ki}-b_{ki}\cos(b_{ki}+d_{ki})q_k\right)+$$

$$+9\sin b_{ki}q_k\cos(b_{ki}-3c_{ki})q_k\left(b_{ki}-\sin(b_{ki}-3c_{ki}+3d_{ik})q_k\right)-$$

$$-\frac{d_{ki}}{d_{ki}+c_{ki}}\tan(b_{ki}-c_{ki})q_k-\sin(b_{ki}-c_{ki})q_k\cos(b_{ki}+c_{ki})q_k+.....\Bigg]+$$

$$+\frac{a_{ki}^5}{b_{ki}\left(1+a_{ki}^2\right)^2}\Bigg[\frac{d_{ki}+3c_{ki}}{12}\Bigg(\frac{c_{ki}}{d_{ki}+c_{ki}}\sin(3b_{ki}-d_{ki})q_k+$$

$$+\frac{3c_{ki}}{d_{ki}+c_{ki}}\sin(b_{ki}-c_{ki}+3d_{ki})q_k+.....\Bigg)-\cos(b_{ki}+3d_{ki})q_k-$$

$$-\frac{d_{ki}+c_{ki}-3e_{ki}}{3}\sin^2(b_{ki}-c_{ki}+2d_{ki}+3e_{ki})q_k-$$

$$-\frac{b_{ki}+3e_{ki}}{d_{ki}+c_{ki}+e_{ki}}\cot(b_{ki}+c_{ki}-d_{ki}-e_{ki})q_k+.....\Bigg], \qquad (6)$$

where the parameters $a_{ki}, b_{ki}.... \; k=1,2,...,12$, $i=$PAM, PAL, FPM, FPL, FCM, FCL, TPM and TPL, depend on measured data in patella (PAM and PAL), femur (patellar surfaces PAM and FPM and condyles FCM and FCL) and tibia (TPM and TPL).

These coeficients are determined by using a genetic algorithm. The experimental data is available in [11].

Figure 5 displays the forces in ligaments and tendons during flexion for an healthy knee for which $\delta\mathbf{A}$ is zero.

The forces in ACL, PCL, MCL, LCL and PTL are represented with respect to the flexion angle.

The peaks are touched in PTL and ACL on 54.25° and 68°, respectively. The smallest forces appear in MCL. LCL reaches the maximum at 73.5°, and PCL at 82.5°. The translation degrees of freedom during flexion are presented in Fig. 6. Translations (except for q_2) are increasing functions relative to the flexion angle.

The q_2 starts to decrease in the vicinity of 78.75° and seems to be a constant in vecinity of 45°.

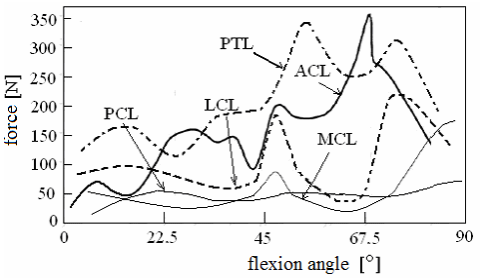

Fig. 5 – Forces in ligaments and tendons during flexion for an intact knee.

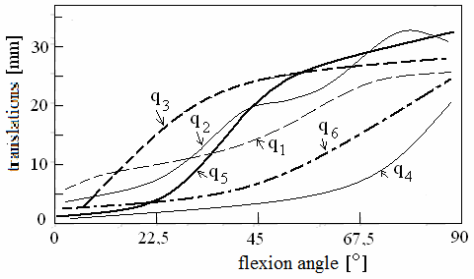

Fig. 6 – Translation degrees of freedom for an intact knee.

The forces in ligaments and tendons during extension for an intact knee are presented in Fig. 7. PTL and ACL have the highest peaks at 54.25° and 68°, respectively. The lowest forces are found for MCL. The LCL reaches its maximum value at 73.5°, while PCL at 82.5°.

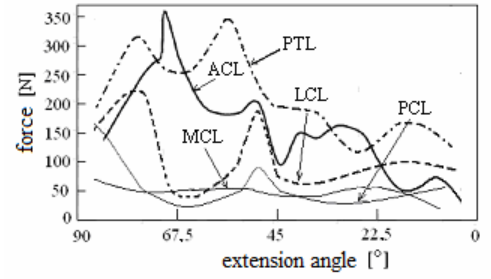

Fig. 7 – Forces in ligaments and tendons during extension for an intact knee.

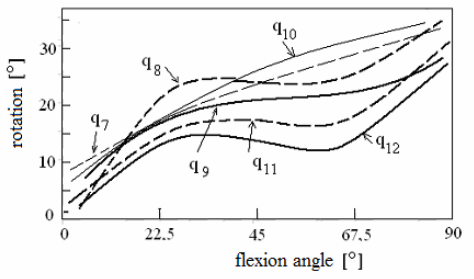

Fig. 8 – Rotation degrees of freedom for an intact knee.

These values are symmetrically with respect to the results obtained for flexion. Figure 8 presents the rotational degrees of freedom for an intact knee. The rotations are increasing functions relative to the flexion angle. The other degrees of freedom have growing and decreasing zones relative to the angle of flexion. The forces in cartilages PAM, PAL, FPM, FPL, FCM, FCL, TPM and TPL during flexion and extension for a normal knee are presented in Fig. 9 and Fig. 10, respectively. These forces are calculated from (6).

We see that the stiffest of cartilage is located in the lateral condyle of the femur FPL for both flexion and extension. The softest cartilage is found in the medial plateau of the tibia TPM for both flexion and extension. The cartilage stiffness was found to be higher in the FPM, PAM, PAL than in FCM, FCL, TPM. In the patella, the medial face is stiffer than the lateral side. In the patellar groove of the femur the lateral face is stiffer than the medial counterpart. In the femoral condyles, the lateral side was stiffer than the medial, which was not found in the tibial plateau.

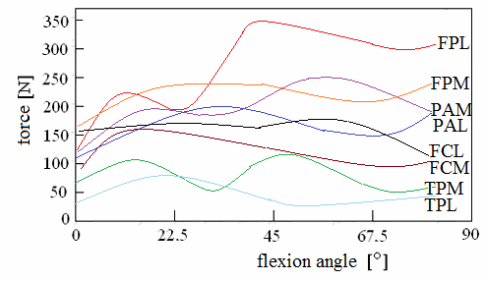

Fig. 9 – Forces in the intact cartilages during flexion.

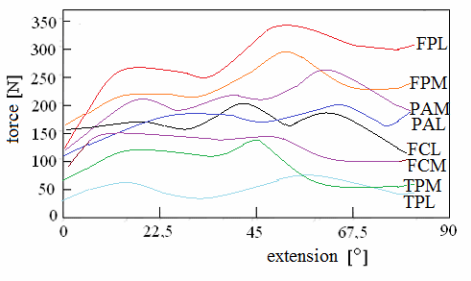

Fig. 10 – Forces in the intact cartilages during extension.

4. THE CASE OF A DAMAGED CARTILAGE

To describe a damaged cartilage in terms of $\delta\mathbf{A}$, the vibration images of a normal/damaged cartilage from patella (PAM and PAL), smoothed by cubic B-splines, are analyzed. Two frequencies of vibration 30 Hz and 60 Hz were used in the sonoelastic approach [17].

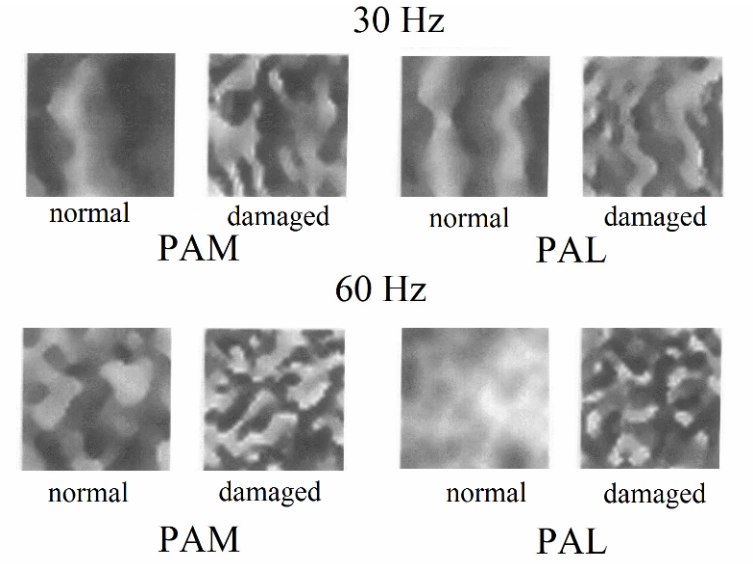

Fig. 11 – Amplitude vibration images representative for normal/ damaged cartilage from patella (PAM and PAL) [17].

Figure11 displays on the right image the normal cartilage and in the left image the damaged cartilage in patella (PAM and PAL). To characterize this damaged cartilage, we tried different values for the diagonal matrix $\delta\mathbf{A}$. The best attempt has stopped to the diagonal values equal 0.05.

As before, the forces in ACL, PCL, MCL, LCL and PTL are represented with respect to the flexion angle. Fig. 12 displays the forces in ligaments and tendons during flexion for a damaged knee for which $\delta\mathbf{A}$ is not zero.

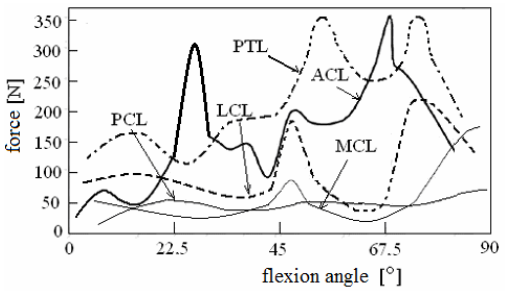

Fig. 12 – Forces in ligaments and tendons during flexion for a damaged knee.

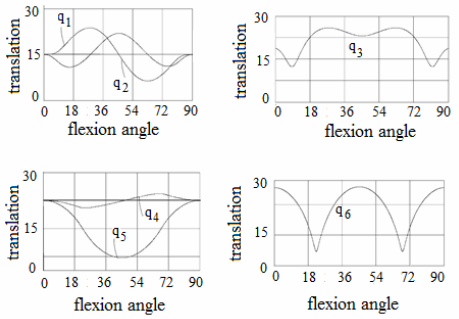

Fig. 13 – Translation degrees of freedom for a damaged knee.

The peaks in PTL and ACL are increased in values, and PTL displays a new peak at 69.2°. The ACL has also a new peak at 24.1°.

Similar changes take place for the extension case. The change in variation of degrees of freedom is dramatically. The evolution of four translation degrees of freedom during flexion are presented in Fig. 13. The translations become oscilating functions relative to the flexion angle.

The same dramatic changes take place for rest of degrees of freedom. In intact cartilage, the echo duration is not different in the zones of measurements, and the damaged cartilage, in contrast, the echo duration is different for zones of measurements [17].

5. CONCLUSIONS

We want to compare our results with the results of other authors in characterizing the elasticity of the human knee joint cartilage. Our study refers to normal cartilage stiffness. The stiffness of the cartilage is evaluated by measurements done one on the medial and lateral faces of the patella, the medial and lateral faces on the patellar surface of the femur, and the medial and lateral femoral condyles and tibial plateau. These measurements we use in this article are available in [11]. So, we obtain that the cartilage stiffness was found to be higher in the FPM, PAM, PAL than in FCM, FCL, TPM. In the patella, the medial face is stiffer than the lateral side. In the patellar groove of the femur the lateral face is stiffer than the medial counterpart. In the femoral condyles, the lateral side was stiffer than the medial, which was not found in the tibial plateau.

In [17] and [18] was found that the stiffest cartilage is in femoral condyles, and the patellar surface of femur is softer. Also, the above-mentioned article found

that the softest cartilage is the tibial plateau. In [17], the lateral condyle was found to be softer in the femur and the medial plateau in the tibia. The latter corresponds with our results. In their studies, no stiffness measurements were made in the patellar cartilage. In [19], the authors found that the stiffest cartilage was located in the lateral femoral condyle and the softest cartilage was in the patellar groove of the femur. This is consistent with our results. In [20] the authors show that the cartilage stiffness is higher in the FPM, PAM, PAL than in other locations that correspond to our results.

Received on January 17, 2017

REFERENCES

1. GAO, L., *Sonoelastography: Theory and experiment development*, PhD Thesis, University of Rochester, Rochester, NY, 1995.
2. GAO, L., PARKER, K.J., ALAM, S.K., LERNER, R.M., *Sonoelasticity imaging: Theory and experimental verification*, J. Acoust. Soc. Am., **97**, *6*, pp. 3875–3886, 1995.
3. PARKER, K.J., LERNER, R.M., *Sonoelasticity of organs: Shear waves ring a bell*, J. Ultrasound Med., **11**, *8*, pp. 387–392, 1992.
4. GAO, L., PARKER, K.J., ALAM, S.K., RUBENS, D., LERNER, R.M., *Theory and Application of Sonoelasticity Imaging*, International journal of imaging systems and technology, Special Issue: Acoustical Tomography, **8**, *1*, pp.104–109, 1997.
5. MOŞNEGUTU, V., IOAN, R., CHIROIU, V., *Two inverse problems for the human knee*, in: *Inverse Problems and Computational Mechanics*, Vol. 1, Editura Academiei Române, Bucharest, pp. 241–258, 2011.
6. MOSNEGUTU, V., CHIROIU.V., *Introducere în modelarea matematică a genunchiului*, Editura Academiei Române, 2013.
7. MOŞNEGUŢU, V., CHIROIU, V., *On the dynamics of systems with friction*, Proceedings of the Romanian Academy, Series A: Mathematics, Physics, Technical Sciences, Information Science, **11**, *1*, pp. 63–68, 2010.
8. CHIROIU, V., MOSNEGUTU, V., MUNTEANU, L., IOAN, R., *On a micromorphic model for the synovial fluid in the human knee*, Mechanics Research Communications, **37**, *2*, pp. 246–255, 2010.
9. ZHENG, N., FLEISIG, G.S., ESCAMILLA, R.F., BARRENTINE, S.W., *An analytical model of the knee for estimation of internal forces during exercise*, J. of Biomechanics, **31**, *10*, pp. 963–967, 1998.
10. HOLEN, J., WAAG, R.C., GRAMIAK, R., *Representations of rapidly oscillating structures on the Doppler display*, Ultrasound Med. Biol., **11**, *2*, pp. 267–272, 1985.
11. LYYRA, T., KIVIRANTA, I., VAATAINEN, U., HELMINEN, H.J., JURVELIN, J.S., *In vivo characterization of indentation stiffness of articular cartilage in the normal human knee*, Journal of Biomedical Materials Research Part A, **48**, *4*, pp. 482–487, 1999.
12. LYYRA, T., *Development, validation and clinical application of the indentation technique for the arthroscopic measurement of cartilage stiffness*, PhD Thesis, Kuopio University, Finland, 1997.
13. LYYRA, T., LINDGREN, R., KAIPIO, J., VAUHKONEN, M., KIVIRANTA, I., JURVELIN, J., *Numerical validation of arthroscopic cartilage stiffness measurement using a finite element model*, Med. Biol. Eng. Comp., **34** (Suppl, Part I), pp. 173–174, 1996.
14. LYYRA, T., AROKOSKI, J., VIHKO, A., *Experimental validation of the arthroscopic cartilage stiffness measurement by enzymatically degraded cartilage samples*, Phys. Med. Biol., **44**, *2*, pp. 525–535, 1999.

15. TOMA, I., *Metoda echivalenței liniare şi aplicațiile ei în mecanică*, Editura Tehnică, Bucharest, 2008.
16. MUNTEANU, L., DONESCU, St., *Introduction to Soliton Theory: Applications to Mechanics*, Book Series Fundamental Theories of Physics, Vol. 143, Kluwer Academic Publishers, Dordrecht, Boston (Springer Netherlands), 2004.
17. University of Rochester School of Medicine and Dentristy, Dept of Orthopedics, Division of Rehabilitation Medicine, NY 14642, *Private report*, 2016.
18. SWANN, A.C., SEEDHOM, B.B., *The stiffness of normal articular cartilage and the predominant acting stress levels: implications for the aetiology of osteoarthrosis*, Br. J. Rheumatol., **32**, *1*, pp. 16–25, 1993.
19. YAO, J.Q., SEEDHOM B.B., *Mechanical conditioning of articular cartilage to prevalent stresses*, Br. J. Rheumatol., **32**, *11*, pp. 956–965, 1993.
20. ATHANASIOU, K.A., ROSENWASSER, M.P., BUCKWALTER, J.A., MALININ, T.I., MOW, V.C., *Interspecies comparisons of in situ intrinsic mechanical properties of distal femoral cartilage*, J. Orthop. Res., **9**, *3*, pp. 330–340, 1991.
21. FROIMSON, M.I., RATCLIFFE, A., MOW, V.C., *Patellar cartilage mechanical properties vary with site and biochemical composition*, Trans. Orthop. Res. Soc., **14**, p. 150, 1989.